Fluid Phase Equilibria 440 (2017) 111–121

Contents lists available at ScienceDirect

Fluid Phase Equilibria

journal homepage: www.elsevier.com/locate/fluid

Predicting the phase behavior of fluorinated organic molecules using the GC-SAFT-VR equation of state

Jessica D. Haley [a, b], Clare McCabe [a, b, c, *]

[a] Department of Chemical and Biomolecular Engineering, Vanderbilt University, Nashville, TN, United States
[b] Multiscale Modeling and Simulation (MuMS) Center, Vanderbilt University, Nashville, TN, United States
[c] Department of Chemistry, Vanderbilt University, Nashville, TN, United States

ARTICLE INFO

Article history:
Received 9 October 2016
Received in revised form
13 December 2016
Accepted 13 January 2017
Available online 20 January 2017

Keywords:
Phase equilibrium
Heteronuclear
Group contribution
Pure fluid
Binary mixture
Perfluoroalkanes
Perfluoroalkylalkanes
Hydrofluoroethers
Carbon dioxide
Fluoroalkanes
Alkanes
Vapor liquid equilibrium
Liquid-liquid equilibrium

ABSTRACT

Fluorinated molecules such as perfluoroalkanes (PFA), perfluoroalkylalkanes (PFAA), fluoroalkanes, and hydrofluoroethers (HFE) possess attractive physical properties that have resulted in their use in a wide range of applications. However, while there is an abundance of thermophysical data for hydrocarbons in the literature, only limited studies have been performed that report the properties of the corresponding fluorinated species. Predictive approaches are therefore needed to accurately and reliably determine the physical properties of these molecules. The statistical associating fluid theory (SAFT) is a commonly used molecular-based equation of state that in its various forms has been applied to study a wide range of fluid systems. In recent work, several group contribution (GC) SAFT equations of state have been proposed, such as the GC-SAFT-VR equation that combines the SAFT equation for potentials of variable range (VR) with a group contribution approach that uniquely allows for the description of hetero-segmented chains. The GC-SAFT-VR equation has been shown to provide an excellent description of the phase behavior of pure associating and non-associating fluids and their mixtures, with a minimal reliance on fitting the model parameters to experimental data. Specifically, parameters for key functional groups (such as CH_3, CH_2, CH, CH_2=CH, C=O, C_6H_5, ether and ester, OH, NH_2, CH=O, COOH) have been obtained by fitting to experimental vapor pressure and saturated liquid density data for selected low molecular weight fluids and then used to predict the phase behavior of pure fluids and their mixtures without further adjusting the group parameters. To expand upon this effort, here we report parameters for the CF_3, CF_2, CF, CH_2F, CHF_2, and CHF functional groups and their cross interactions. The theoretical predictions are compared with experimental data for pure PFAs, PFAAs, and HFEs, as well as binary mixtures of alkanes, alkenes, PFAs, PFAAs, and CO_2 in order to test the transferability of the new group parameters. The GC-SAFT-VR approach is found to accurately predict the phase behavior of the systems studied.

1. Introduction

Fluorinated molecules possess unique characteristics that have proven to be useful in various applications [1,2]. Many of their advantageous properties, including low surface tension, high fluidity, low dielectric constant, high vapor pressure and compressibility, gas solubility, and excellent spreading properties, are due to the overlapping of orbitals in the C-F bonds and the dense electron cloud of the fluorine atoms that protects the chain against reagents. Consequently, fluorinated molecules tend to be chemically and biologically inert and manipulating the structure of organic molecules to include fluorination can introduce dramatically different and often desirable properties.

The simplest of the organofluorine molecules are the perfluoroalkanes (PFA), which are hydrocarbons in which all the C-H bonds are replaced by C-F bonds. Despite the significantly higher molecular weight for PFAs as compared to the corresponding alkane, the boiling points of PFAs are surprisingly similar to those of the corresponding alkanes. This phenomenon suggests that the intermolecular forces between PFA molecules are relatively weak and are also responsible for the high ionization potential and low polarizability of PFA molecules. However, PFA molecules exhibit strong intramolecular bonds that result in excellent spreading properties, high viscosity, immiscibility with hydrocarbons and

* Corresponding author. Department of Chemical and Biomolecular Engineering, Vanderbilt University, Nashville, TN, United States.
E-mail address: c.mccabe@vanderbilt.edu (C. McCabe).

http://dx.doi.org/10.1016/j.fluid.2017.01.013
0378-3812/

water, as well as low refractive index. PFAs also exhibit high solubility in CO_2 and oxygen, which has led to their use in several environmental applications, including the removal of CO_2 from gaseous effluents, the design of CO_2-philic surfactants, and in medical applications such as oxygen carriers in artificial blood substitutes [2–4].

A second unique type of fluorinated molecules are the perfluoroalkylalkanes (PFAA) which consist of an alkyl chain bonded to a perfluorinated chain with general structure $F(CF_2)_n(CH_2)_mH$. The dual nature of the PFAA structure results in a molecule with amphiphilic character [5], which contributes to many of the distinctive properties that PFAAs exhibit. Additionally, there is a marked difference in the electronegativity of the hydrocarbon side and the fluorinated side of the molecule that leads to a dipole moment along the molecular backbone [6,7]. These characteristics, along with the fact that PFAAs are thermally, chemically, and biologically inert, have led to a wide range of applications for these molecules, including use as excipients for inhalative liquid drug carrier systems [8], surface-active agents, temporary blood substitutes and eye replacement fluids [9], as well as dewetting and lubricating compounds [1]. In this work, PFAA molecules will be referred to using the F_xH_y nomenclature, where x refers to the number of perfluorinated carbon atoms and y refers to the number of hydrogenated carbon atoms in the PFAA molecule.

Another interesting class of fluorinated molecules that we consider are the dipolar hydrofluoroethers (HFEs) with the structure R_X-O-R_Y where R_X and R_Y represent distinctive chains attached to the oxygen atom. Hydrofluoroethers along with hydrofluorocarbons are used as environmentally friendly alternatives to chlorofluorocarbons and hydrochlorofluorocarbons and as such many industrial and commercial applications (e.g. cleaning solvents, refrigerants, foaming agents, carrier solvents for coatings, and lubricants) utilize HFEs [10].

Despite the proven usefulness of these organofluorine molecules, only limited work has been done to experimentally characterize their thermodynamic properties and phase behavior. As a result, the accurate calculation of thermodynamic properties from cubic equations of state is difficult since such equations tend to be heavily reliant on experimental data for parameter estimation. Statistical mechanics based equations of state are an appealing alternative since they usually have more predictive ability by taking into account the effects of molecular shape, size, and interactions on the thermodynamic properties. The statistical associating fluid theory (SAFT) [11,12], based on Wertheim's first order thermodynamic perturbation theory [13–16], is one such approach and has been used by several authors to study fluorinated systems. In perhaps the first study, Archer et al. [17], utilized the bonded hard-sphere (BHS) theory, which models molecules as chains of tangentially bonded hard-spherical segments that interact through a mean field dispersion term, to examine the critical behavior of the perfluoroalkane homologous series. The BHS approach was found to predict the correct trend in critical point for the perfluoroalkane series as well as upper critical solution temperatures (UCSTs) of alkane and perfluoroalkane mixtures. Subsequently, M^{c}Cabe et al. [18] studied the high-pressure phase behavior and critical lines of perfluoromethane + n-alkanes (C1–C8) and the symmetric alkane + perfluoroalkane mixtures from C_1-C_4 utilizing the SAFT-VR equation and pure component parameters proposed by Gil-Villegas [19]. A single binary interaction parameter was fitted to the high-pressure critical line for the perfluoromethane + butane system and found to be transferable to mixtures of similar chain lengths; however, it was observed that as the alkane chain length increased the deviation between the theoretical predictions and experiment increased. Therefore, a different binary interaction parameter was used for mixtures containing longer alkane chains. In related work with the SAFT-VR approach, Morgado et al. [20] studied the low-pressure liquid-liquid immiscibility behavior of alkane + PFA binary mixtures with chain lengths of 5–8 carbon atoms. A new set of binary interaction parameters was proposed, based on reproducing the UCST and excess volumes of the n-hexane + n-perfluorohexane system, and then used transferably to predict the vapour–liquid equilibria, liquid–liquid equilibria and excess volumes of other binary mixtures without additional fitting to experimental data. Using the soft-SAFT equation for homonuclear LJ chain fluids, Dias et al. [21] examined the solubility of xenon and oxygen in perfluoroalkanes as well as the vapor-liquid and liquid-liquid equilibrium of n-alkane + n-perfluoroalkane mixtures. A single cross interaction parameter was introduced to model the phase behavior of the n-perfluoroalkanes + n-alkanes of similar chain lengths; however, for the binary mixtures of xenon and oxygen with perfluoroalkanes, binary interaction parameters were adjusted for each mixture. In a later combined experimental and theoretical study [22], the phase behavior of carbon dioxide and PFA mixtures was investigated using a modified soft-SAFT equation that included quadrupolar interactions for carbon dioxide, perfluorobenzene, and perfluorotoluene. In comparison to the original soft-SAFT equation, the approach was found to provide good agreement with experimental data without the use of fitted binary interaction parameters for mixtures involving fluorinated aromatic compounds + carbon dioxide; however, the results obtained for carbon dioxide + other non-aromatic fluorinated molecules were not affected by the addition of the quadrupolar contribution and still required the optimization of binary interaction parameters.

Turning to PFAA molecules, Morgado et al. [23] used the so called hetero-statistical associating fluid theory for potentials of variable range (hetero-SAFT-VR) [24,25], to study, the density and molar volumes of perfluorohexylhexane (F_6H_6) and perfluorohexyloctane (F_6H_8). The hetero-SAFT-VR approach enables the PFAAs to be described as diblock molecules, i.e., formed from two different chains of tangentially bonded segments representing the perflouroalkyl and alkyl parts of the molecules with different size and/or energy parameters. The alkyl and perflouroalkyl segments were described using parameters for the alkanes and perfluoroalkanes developed in earlier work [20,25] and a binary interaction parameter fitted to the hexane + perfluorohexane binary mixture. Using this approach, experimental densities were predicted within 1% at atmospheric pressure and 3.5% for higher pressures. In a later study [26], the molar volumes and partial molar volumes at infinite dilution of PFA and PFAA molecules in n-octane were predicted, again utilizing the hetero-SAFT-VR approach. Using the same parameters and molecular model as the previous study [23], the molar volume and partial molar volumes at infinite dilution of the PFA molecules were found to have deviations from experiment of less than 5% in all cases. The theoretical results for PFAAs in n-octane were found to be slightly better than those found for the PFAs, with deviations between 0.1% and 2.5%. Following the approach proposed by Morgado [23], dos Ramos et al. [28] also utilized the hetero-SAFT-VR approach to examine the phase equilibria of binary mixtures of n-alkanes, PFAs, and PFAAs. The effect of the molecular weight of the n-alkanes and PFAs on the type of phase behavior observed in these mixtures was studied; however, experimental data was not available and so the accuracy of the theoretical predictions could not be tested.

Hydrofluoroethers (HFEs) have also been studied previously using the SAFT family of equations. In an experimental and theoretical study, Lafitte et al. [29] utilized the SAFT-VR Mie equation of state to model and characterize pure hydrofluoroethers. Molecular parameters were determined for the HFEs studied by fitting to heat of vaporization, experimental normal boiling point, compressed liquid density, and speed of sound data

for methyl perfluorobutyl ether (HFE–7000), 2-trifluoromethyl-3-ethoxydodecafluorohexane (HFE-7500), methyl nonafluorobutyl ether (HFE - 7100), and ethyl nonafluorobutyl ether (HFE - 7200). Deviations between theoretical results and experimental data of less than 4% were found in all cases. Saturation pressure, saturated liquid density, isobaric heat capacity, thermal expansivity, and speed of sound data were then predicted at conditions not considered during the fitting procedure. Although, exact deviations were not provided, the theoretical predictions were found to be in good agreement with the available experimental data. Pure HFEs have also been studied using the perturbed-chain SAFT (PC-SAFT) equation of state by Vijande et al. [30]. The model parameters were optimized against compressed and saturated liquid densities at several temperatures and pressures and then used to predict the saturation pressure with good results. A group-contribution like approach was also proposed that enables the model parameters to be extrapolated and used to predict the saturation pressure and liquid density of other molecules in the same family.

In present work, to characterize both pure PFA, PFAA, and HFE fluids along with their mixtures, the GC-SAFT-VR equation is used [31]. The GC-SAFT-VR equation combines the SAFT-VR [19] equation with a group contribution (GC) [31] approach that allows for the description of chains built up from segments of different size and/or energy of interaction. This approach allows for the location of the functional groups and association sites within a molecule to be specified, enabling the heterogeneity in molecular structure to be captured within a SAFT model. An advantage of the GC-SAFT-VR approach, when the groups of interest are present in a single molecule, is the ability to determine group cross-interaction parameters using pure fluid experimental data for molecules containing the groups of interest (i.e., the cross parameters need not be adjusted to mixture experimental data). In earlier work, GC-SAFT-VR parameters were determined for a wide range of functional groups that allow the phase behavior of compounds such as alkanes, linear and branched alkenes, ketones, acetates, esters, alcohols, aldehydes, amines, carboxylic acids , aromatics, and polymers to be studied [7, 31–36]. In this work, GC-SAFT-VR molecular parameters are determined for the CF_3, CF_2, CF, CHF, CH_2F, and CHF_2 functional groups for selected fluoroalkanes, PFAs, and PFAAs using simulated annealing [37] as in prior work to fit the model parameters to experimental data. The transferability of the group parameters determined is then examined by predicting the phase behavior of molecules not included in the fitting process and the phase behavior of mixtures. Specifically mixtures of PFAs and PFAAs molecules with each other, and with carbon dioxide, hydrofluoroethers, alkanes, and alkenes have been studied.

The remainder of the paper is organized as follows: the molecular model and theory are presented in Section 2, the functional group parameter estimation and results for both pure fluids and mixtures are discussed in Section 3, and conclusions drawn in Section 4.

2. Models and theory

The GC-SAFT-VR approach models fluids as chains composed of tangentially bonded segments that represent the functional groups within the molecule [25,31]. The segments representing each functional group interact via the square well potential, which can be described by,

$$u_{ki,lj}(r) = \begin{cases} +\infty & \text{if} \quad r < \sigma_{ki,lj} \\ -\varepsilon & \text{if} \quad \sigma_{ki,lj} \le r \le \lambda_{ki,lj}\sigma_{ki,lj} \\ 0 & \text{if} \quad r \le \lambda_{ki,lj}\sigma_{ki,lj} \end{cases} \tag{1}$$

here $u_{ki,lj}$ represents the interaction between a functional group of type i present in molecule k with a functional group of type j in molecule l, σ is the segment diameter, ε is the depth of the square well, λ is the potential range, and r is the distance between the two groups. The unlike size and energy interactions can be obtained from the Lorentz-Berthelot combining rules expressed by,

$$\sigma_{ij} = \frac{\sigma_{ii} + \sigma_{jj}}{2} \tag{2}$$

$$\varepsilon_{ij} = \sqrt{\varepsilon_{ii}\varepsilon_{ij}} \tag{3}$$

and the unlike potential range is given by,

$$\lambda_{ij} = \frac{\lambda_{ii}\sigma_{ii} + \lambda_{jj}\sigma_{jj}}{\sigma_{ii} + \sigma_{jj}} \tag{4}$$

As discussed above, for interactions involving polar functional groups which are expected to deviate from the Lorentz-Berthelot combining rules, the unlike interactions between functional groups can be adjusted by fitting to pure component experimental data for molecules containing the functional groups of interest. As such, a predictive equation for the study of mixture phase behavior is retained.

Within the GC-SAFT-VR approach, the free energy is written as the sum of four separate contributions:

$$\frac{A}{Nk_BT} = \frac{A^{ideal}}{Nk_BT} + \frac{A^{mono}}{Nk_BT} + \frac{A^{chain}}{Nk_BT} + \frac{A^{assoc}}{Nk_BT} \tag{5}$$

where N is the total number of molecules in the system, T is the temperature, k_B is the Boltzmann constant, A^{ideal} is the ideal free energy, A^{mono} is the contribution to the free energy due to the monomer segments, A^{chain} is the contribution due to the formation of bonds between monomer segments, and A^{assoc} is the contribution due to association. The expressions for A^{assoc} are not included in this work since the systems studied are not associating fluids. The expressions for each of the remaining terms for a mixture system composed of heteronuclear chain molecules are presented below. Since the theory has been well documented [31,38] only a brief description of the important expressions are provided below.

The ideal Helmholtz free energy is given by,

$$\frac{A^{ideal}}{Nk_BT} = \sum_{k=1}^{n_{components}} x_k \ln\left(\rho_k \Lambda_k^3\right) - 1 \tag{6}$$

where $n_{components}$ represents the number of pure components, $\rho_k = N_k/V$ (the molecular number density of chains of component k), x_k is the mole fraction of component k in the mixture, and Λ_k is the thermal de Broglie wavelength of component k.

The monomer free energy is given by a second order high temperature expansion using Barker and Henderson perturbation theory for mixtures [39],

$$\frac{A^{mono}}{Nk_BT} = \sum_{k=1}^{n} \sum_{i=1}^{n'_k} m_{ki} x_k \left(a^{HS} + \frac{a_1}{k_BT} + \frac{a_2}{(k_BT)^2}\right) \tag{7}$$

where n'_k is the number of types of functional groups i in a chain of component k and m_{ki} the number of segments of type i in chains of component k. a^{HS} is the hard-sphere reference term, and a_1 and a_2 are the first and second perturbation terms, respectively.

Finally, the free energy due to chain formation is given by,

$$\frac{A^{chain}}{NkT} = -\sum_{k=1}^{n} x_k \sum_{ij} \ln y_{ki,kj}^{SW}\left(\sigma_{ki,kj}\right) \tag{8}$$

where the first sum is over all components in the mixture and the second sum considers the chain formation and connectivity of the segments within a given chain k. The background correlation function $y_{ki,kj}^{SW}$ is given by,

$$y_{ki,kj}^{SW}\left(\sigma_{ki,kj}\right) = \exp\left(\frac{-\varepsilon_{ki,kj}}{k_B T}\right) g_{ki,kj}^{SW}\left(\sigma_{ki,kj}\right) \tag{9}$$

where $g_{ki,kj}^{SW}(\sigma_{ki,kj})$ is the radial distribution function for the square well monomers at the contact distance $\sigma_{ki,kj}$ and is approximated by a first-order high-temperature perturbation expansion.

Thermodynamic properties, such as the pressure and chemical potential can then be obtained from the summation of the Helmholtz energy using standard thermodynamic relationships.

3. Results and discussion

Molecular parameters for six new functional groups (CF_3, CF_2, CF, CH_2F, CHF_2, and CHF) within the GC-SAFT-VR approach have been determined by fitting to experimental data [30,40] for selected members of the different chemical families that contain these functional groups, e.g., PFAs, PFAAs, and HFEs. For each chemical family studied, a representative sample of molecules for which experimental vapor pressure and saturated liquid density data is available was chosen for the fitting process, while some pure compounds were reserved to test the ability of the approach to accurately predict phase behavior and thus illustrate the transferability of the group parameters. Data close to the triple point of the fluids were excluded from the fitting process since the inclusion of such data has been shown to skew the results [41]. In addition, data near the critical point was also excluded from the fitting process since the GC-SAFT-VR approach, like all analytical equations of state, does not consider the long-range density fluctuations that occur in the critical region and over predicts the critical pressure and temperature of the fluid [42]. Additionally, the lowest members of the homologous series were excluded from the study since their properties typically deviate from the behavior exhibited by the longer chained members [31]. The molecular parameters (m_{ki}, $\sigma_{ki,lj}$, $\varepsilon_{ki,lj}$, and $\lambda_{ki,lj}$) for each new functional group are reported in Tables 1–3.

3.1. Pure fluids

In the GC-SAFT-VR approach, perfluoroalkanes are described by the CF_3 and CF_2 functional groups. In order to reduce the number of fitted parameters for the fluorinated groups, the relationship proposed by Archer [17] for m was used, which yields $m_{CF_3} = 0.685$ and $m_{CF_2} = 0.370$. The 3 remaining parameters ($\sigma_{ki,lj}$, $\varepsilon_{ki,lj}$, and $\lambda_{ki,lj}$) were determined by fitting to experimental vapor pressure and saturated liquid density data for perfluorobutane (C_4F_{10}), perfluoropentane (C_5F_{12}), perfluoroheptane (C_7F_{16}), perfluorooctane (C_8F_{18}), and

Table 1
GC-SAFT-VR parameters for the segment size σ and segment number, m, of each functional group studied.

Groups	σ (Å)	m_i
CF_3	4.618	0.685
CF_2	4.345	0.370
CF_2 α	4.345	0.370
CF	3.251	0.269
CHF_2	3.076	1.577
CH_2F	3.338	1.046
CHF	3.962	0.548

Table 2
GC-SAFT-VR segment-segment dispersion energy range parameters $\lambda_{ki,lj}$.

	CF_3	CF_2α	CF_2	CF	CHF_2	CH_2F	CHF
CH_3	1.398	1.572	1.572	1.644	1.421	1.463	1.421
CH_2	1.483	1.819	1.654	1.734	1.524	1.560	1.512
CH	1.608	1.786	1.786	1.888	1.678	1.709	1.649
C=O	1.567	1.752	1.752	1.856	1.631	1.666	1.606
CH_2=CH	1.429	1.303	1.303	1.687	1.461	1.501	1.455
C_6H_5	1.605	1.801	1.801	1.918	1.683	1.717	1.650
OCH_2 (esters)	1.435	1.630	1.630	1.721	1.472	1.516	1.465
OCH_3 (esters)	1.455	1.647	1.647	1.739	1.495	1.538	1.486
OCH (esters)	1.323	1.508	1.508	1.575	1.330	1.379	1.341
cis-CH=CH	1.563	1.752	1.752	1.858	1.628	1.663	1.602
trans CH=CH	1.534	1.721	1.721	1.820	1.592	1.628	1.571
OCH_3 (ether)	1.423	1.611	1.611	1.695	1.455	1.498	1.450
OCH_2 (ether)	1.597	1.621	1.621	1.755	1.468	1.555	1.547
OCH (ether)	1.628	1.848	1.848	1.990	1.723	1.760	1.680
C-CH_2	1.590	1.782	1.782	1.893	1.663	1.697	1.633
OH terminal	1.414	1.561	1.561	1.618	1.436	1.470	1.435
OH internal	1.700	1.838	1.838	1.919	1.765	1.786	1.736
CH=O	1.410	1.586	1.586	1.659	1.437	1.478	1.435
NH_2	1.413	1.606	1.606	1.692	1.443	1.489	1.440
NH	1.497	1.678	1.678	1.767	1.544	1.581	1.529
COOH	1.431	1.643	1.643	1.747	1.470	1.519	1.463
C_6H_6	1.489	1.675	1.675	1.768	1.536	1.575	1.521
CO_2	1.398	1.597	1.597	1.684	1.426	1.474	1.425
CF_3	1.321	1.591	1.591	1.526	1.327	1.367	1.336
CF_2α	1.476	1.641	1.641	1.717	1.515	1.549	1.504
CF_2	1.476	1.641	1.641	1.717	1.515	1.549	1.504
CF	1.526	1.717	1.717	1.818	1.584	1.621	1.563
CH_2F	1.367	1.549	1.549	1.621	1.385	1.430	1.389
CHF_2	1.327	1.515	1.515	1.584	1.336	1.385	1.346
CHF	1.336	1.504	1.504	1.563	1.346	1.389	1.354

Table 3
GC-SAFT-VR segment-segment dispersion energy well depth parameters $\varepsilon_{ki,lj}/k_B$ (K).

	CF_3	CF_2α	CF_2	CF	CHF_2	CH_2F	CHF
CH_3	271.88	226.43	226.43	260.40	258.13	253.82	328.97
CH_2	273.60	227.87	177.96	262.05	259.77	255.43	331.05
CH	177.65	147.95	147.95	170.15	168.67	165.85	214.95
C=O	356.58	296.97	296.97	341.51	338.54	332.89	431.45
CH_2=CH	263.09	166.52	166.52	251.97	249.78	245.61	318.33
C_6H_5	192.11	160.00	160.00	184.00	182.40	179.35	232.45
OCH_2 (esters)	183.04	152.44	152.44	175.30	173.78	170.88	221.47
OCH_3 (esters)	221.85	184.76	184.76	212.48	210.63	207.11	268.43
OCH (esters)	160.06	133.31	133.31	153.30	151.97	149.43	193.67
cis-CH=CH	206.28	171.79	171.79	197.56	195.84	192.57	249.59
trans-CH=CH	221.47	184.45	184.45	212.12	210.27	206.76	267.97
OCH_3 (ether)	269.63	224.56	224.56	258.24	255.99	251.72	326.24
OCH_2 (ether)	340.53	191.95	191.95	228.43	224.54	222.66	288.58
OCH (ether)	146.80	122.26	122.26	140.60	139.38	137.05	177.63
C-CH_2	125.61	104.61	104.61	120.30	119.26	117.27	151.98
OH terminal	410.80	342.13	342.13	393.45	390.03	383.52	497.06
OH internal	327.10	272.42	272.42	313.28	310.55	305.37	395.77
CH=O	323.45	269.38	269.38	309.79	307.10	301.97	391.37
NH_2	277.50	231.11	231.11	265.77	263.46	259.07	335.76
NH	441.14	367.40	367.40	422.51	418.83	411.84	533.77
COOH	252.10	209.96	209.96	241.46	239.36	235.36	305.04
C_6H_6	249.82	208.06	208.06	239.27	237.18	233.23	302.27
CO_2	237.87	198.11	198.11	227.83	225.85	222.08	287.82
CF_3	315.56	262.81	262.81	302.23	299.60	294.60	381.81
CF_2α	262.81	218.87	218.87	251.70	249.51	245.35	317.99
CF_2	262.81	218.87	218.87	251.70	249.51	245.35	317.99
CF	302.23	251.70	251.70	289.46	286.94	282.15	365.68
CH_2F	294.60	245.35	245.35	282.15	279.70	275.03	356.45
CHF_2	299.60	249.51	249.51	286.94	284.45	279.70	362.50
CHF	381.81	317.99	317.99	365.68	362.50	356.45	461.98

perfluorodecane ($C_{10}F_{22}$) and using Lorentz Berthelot combining rules to describe the cross interactions. These parameters were then used to predict the phase behavior of perfluoropropane (C_3F_8), perfluorohexane (C_6F_{14}), and perfluorononane (C_9F_{20}). For the correlated PFAs the average deviation in the vapor pressure compared to experiment was found to be 3.86% and for the saturated liquid densities 2.08%, while for the predicted systems the deviations were 6.03% for the vapor pressure and 3.85% for the saturated liquid densities. The percentage absolute average deviations (%AAD) obtained from the GC-SAFT-VR approach for the vapor pressure and saturated liquid densities of each substance studied are reported in Table A.1 of the appendix material.

Due to the polarity of PFAA molecules, the Lorentz Berthelot combining rules do not always accurately capture the cross interactions in these systems. In particular, rather than using the CH_3 and CH_2 parameters determined in earlier work [11] with the CF_3 and CF_2 parameters obtained from fitting to the PFA family as described above, the interaction between the CH_2 and CF_2 groups has been fitted to vapor pressure and saturated liquid density data for perfluorobutylpentane (F_4H_5) and perfluorobutylhexane (F_4H_6). The vapor pressure and saturated liquid densities of perfluorobutyloctane (F_4H_8), perfluorohexyloctane (F_6H_8), and perfluorohexylhexane (F_6H_6) were then predicted. Using this approach we can accurately capture the behavior of the smaller PFAA molecules, giving deviations of 3–4% in vapor pressure and less than 1% for the saturated liquid densities; however, for the larger PFAA molecules, the observed deviations are higher (~10%). Further investigation of the molecular interactions in the PFAA molecules was performed and electron density maps, which measure the probability that an electron is present at a specific location in a molecule, were calculated using GaussView version 5 [43]. As can be seen in Fig. 1, the high electronegativity (4.0 on the Pauling scale) of fluorine results in the fluorine atoms drawing electrons from the adjacent carbon atoms and results in a partial negative charge on the fluorines and a partial positive charge on the carbons. As a representative example of the PFAA molecules studied, Fig. 1 provides an electron density map for F_4H_5. From this we can also see that the electron density is greater for the CH_2 and CF_2 groups at the junction of the perfluorinated and hydrogenated segments of the molecule compared to the remaining CH_2 and CF_2 groups present. Therefore, to better capture the molecular behavior of the PFAA molecules in the GC-SAFT-VR model, two CH_2-CF_2 cross interactions were defined: one for the CH_2-CF_2 group at the junction of the perfluorinated and hydrogenated segments, which we denote as α CH_2-CF_2, and a second general CH_2-CF_2 to describe the interaction with the remainder of the CF_2 groups in the molecule. Utilizing this approach, deviations of less than 1% were obtained in liquid density for all correlations and predictions and 5% for the vapor pressures. The percentage absolute average deviations (% AAD) obtained from the GC-SAFT-VR approach for the vapor pressure and saturated liquid densities are reported in Table A.1 of the appendix material. All of the remaining interactions were determined using standard Lorentz-Berthelot combining rules and are reported in Tables 2 and 3

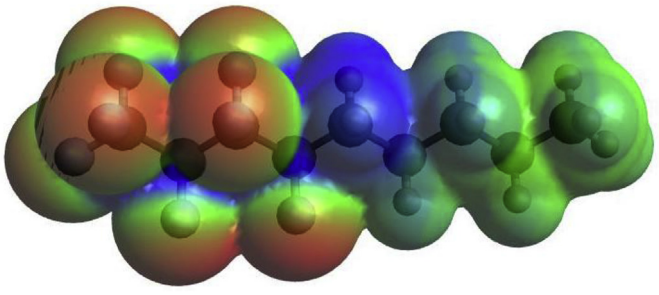

Fig. 1. Electrostatic potential map for perfluorobutylpentane (F_4H_5) created using GaussView version 5 [43]. The red region represents the lowest electrostatic potential data and the blue region represents the highest. (For interpretation of the references to colour in this figure legend, the reader is referred to the web version of this article.)

To describe branched fluorinated molecules, a CF group needs to be defined and parameterized. The parameters for the CF segment were determined by fitting to vapor pressure and saturated liquid density data for the 2-fluoro-2-methylbutane molecule, which is comprised of the CH_3, CH_2, and CF groups. The parameters for the CF group were optimized with the CH_2 and CH_3 group parameters being taken from previous work [31]. We note that very limited experimental data is available for molecules containing a CF group and so testing the resulting model parameters by predicting the phase behavior of other pure components was not possible.

Having developed parameters for all of the alkyl-fluoro (i.e., CF_3, CF_2, and CF) groups, in Fig. 2, we report the molecular parameters obtained for the CF_3, CF_2, and CF groups as a function of molecular weight. As can be seen from the figure the values for, $m\lambda$ and $m\sigma^3$ essentially increase linearly with molecular mass, while for $m\varepsilon/k_B$ the CF_2 and CF groups show similar interaction energy. This deviation from linearity could be due to the non-ideal nature of the interactions seen in systems containing fluorine, since we note a linear trend was observed in previous work for the CH_3, CH_2, and CH functional groups [31].

In addition to the CF group, the CHF_2, CH_2F and CHF groups are also necessary to describe branched fluorinated molecules. To obtain parameters for the CHF_2 group, the 1,1-difluoroalkane family, comprised of the groups CHF_2, CH_2, and CH_3, was studied. Using parameters for the CH_2 and CH_3 groups from previous work [31], parameters were determined for the CHF_2 group by fitting to experimental vapor pressure and saturated liquid density for 1,1-difluoropentane and 1,1-difluorohexane. The phase behavior of 1,1-difluoroheptane and 1,1-difluorooctane were then predicted in order to test the model parameters. The molecules fitted were found to have an average deviation of 6.53% in vapor pressure and 0.098% in liquid density compared to the experimental data, while the predicted molecules exhibited deviations of 9.75% in vapor pressure and 0.127% in saturated liquid density. The %AAD obtained from the GC-SAFT-VR correlations and predictions are reported in Table A.1. Parameters for the CH_2F group were obtained by considering 1-fluoroalkanes, which also contain the CH_3 and CH_2 groups. Parameters for the CH_2F group were determined by fitting to vapor pressure and saturated liquid density data for 1-fluoroheptane and 1-fluorooctane and the phase behavior of 1-fluoropentane, 1-fluorohexane, and 1-fluorononane was then predicted. As reported in Table A.1, the average %AAD between experiment and the GC-SAFT-VR predictions for the vapor pressure and saturated liquid density for was found to be 5.22% and 0.33% respectively. The CHF group is present in 2-fluoroalkanes and 3-fluoroalkanes and so was used to determine the model parameters for this group. Specifically, 3-fluorohexane was used to determine the group parameters by fitting to vapor pressure and saturated liquid density data, while the phase behavior of 3-fluoropropane and 2-fluorobutane was predicted. An absolute average deviation between the experimental data and GC-SAFT-VR predictions of 4.95% in vapor pressure and 1.53% in saturated liquid density was obtained as reported in Table A.1.

Using the molecular parameters determined from the fluorinated group fittings discussed above, the phase behavior of pure HFEs was then studied. HFE molecules are formed using the functional groups CF_3, CF_2, CH_2, CHF, and CHF_2 as defined in this work and the OCH_2 group, the parameters for which were taken from previous work [31]. For example, HFE-347pc-f (CHF_2-CF_2-OCH_2-

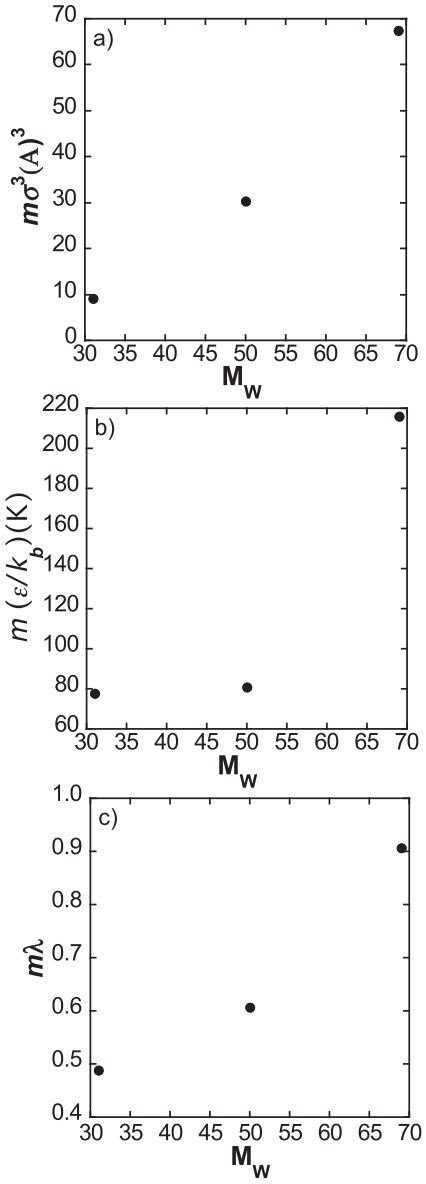

Fig. 2. GC-SAFT-VR molecular parameters for the functional groups CF_3, CF_2, and CF as a function of the molecular weight (M_W): (a) segment size, (b) potential well depth, and (c) potential range.

CF_3) is formed using the four groups CF_3, OCH_2, CF_2 and CHF_2, while HFE-449mec-f (CF_3-CHF-CF_2-OCH_2-CF_3) contains the groups CF_3, OCH_2, CF_2, and CHF. The presence of an ether oxygen, in the molecular backbone typically leads to chain polarity due to the C-O bond [44] and so deviation from Lorentz-berthelot combining rules are to be expected. To address this, the interaction between the ether OCH_2 and fluorinated groups, i.e., OCH_2 and CF_3, OCH_2 and CF_2, OCH_2 and CHF, and OCH_2 and CHF_2 were obtained by fitting to pure component vapor pressure data as follows: The OCH_2 and CF_3 cross interaction was determined by fitting to the vapor pressure of HFE-356mf-f (CF_3-OCH_2-CH_2-CF_3) and a deviation in vapor pressure from the experimental data of 0.21% was obtained. The ether OCH_2 and CF_2, cross interaction was determined by fitting to the vapor pressure of HFE-467mccf (CF_3-CF_2-CF_2-OCH_2-CH_3) and a deviation in vapor pressure of 0.74% was found. The OCH_2 and CHF cross interaction was determined by fitting to the vapor pressure of HFE-449mec-f (CF_3-CHF-CF_2-OCH_2-CF_3) and a deviation in vapor pressure of 7.6% was found. Finally, the cross interaction between the OCH_2 and CHF_2 groups was determined by fitting to the vapor pressure of HFE-347mcf (CF_3-CF_2-OCH_2-CHF_2) and the deviations in vapor pressure were found to be 4.0%. Using these interactions, the vapor pressure of the remaining HFE molecules, HFE-347pc-f (CHF_2-CF_2-OCH_2-CF_3), HFE-374pcf (CHF_2-CF_2-OCH_2-CH_3), HFE-449mcf-c (CF_3-CF_2-OCH_2-CF_2-CHF_2), HFE-458pcf-c (CHF_2-CF_2-OCH_2-CF_2-CHF_2), and HFE-569mccc (CF_3-CF_2-CF_2-CF_2-OCH_2-CH_3), was then predicted and the calculated average deviations from the experimental data found to be 5.7% in vapor pressure. The percentage absolute average deviations (%AAD) obtained from the GC-SAFT-VR approach for the vapor pressures are reported in Table A.1 of the appendix material. Although the deviations reported by Vijande [30] are generally smaller than reported here, we note that in the work of Vijande, the phase behavior of HFE molecules was studied using a more complicated model in which two sets of parameters (based on the connectivity of the molecule) for each of the CH_3, CH_2, CF_3, and CF_2 groups were used to describe the interactions due to chain polarity.

3.2. Binary mixtures

With new molecular parameters for the organic fluorine groups determined, the phase behavior of binary mixtures containing these functional groups can be examined. The phase behavior of perfluoroalkane and alkane binary mixtures were first considered. Although both alkanes and perfluoroalkanes are nonpolar species, and thus it would be expected that their mixtures behave almost ideally, in reality these mixtures display large positive deviations from ideality [45,46], which typically necessitates the fitting of cross interaction parameters to binary mixture data in equation of state studies. However, with the GC-SAFT-VR approach no additional fitting beyond the group parameters already determined is required to predict the phase behavior. In Fig. 3 results are presented for binary mixtures of perfluorohexane + *n*-alkanes pentane, heptane and octane and hexane + perfluoroalkanes, perfluorooctane, perfluoroheptane, perfluorohexane, and perfluoropentane. From the figures, we can see that the theory is able to accurately predict the phase behavior of each binary mixture studied. We note that similar results were observed in the work of Morgado et al. [20] where binary interaction parameters were fitted to UCST and excess volume data for the n-hexane + n-perfluorohexane system. In Fig. 4, we show the *pT* projection of the critical line for the butane (1) + perfluorobutane (2) mixture. Results from the SAFT-VR [18] equation are also shown for comparison and good agreement is found between the two approaches.

Next we predict, again without fitting any cross interaction parameters to mixture data, the phase diagrams of the perfluorohexane + hexane and perfluorohexane + pentane binary mixtures. The *Pxy* phase diagrams at three different constant temperatures slices (318.15 K, 308.15 K, and 298.15 K) are shown in Fig. 5a for perfluorohexane + hexane. We note that this mixture was also studied in the work of Morgado et al. [20], who observed a slight under-prediction in the pressure with the hetero-SAFT-VR approach, and in the work of Colina et al. [47], where SAFT-VR predictions over-predicted the pressure as well as the pure vapor pressure. In our work, using a purely predictive group contribution approach, the theory correctly captures the shape of the curves and results in lower deviations for the vapor pressure than in earlier studies, despite those studies fitting cross interaction parameters to the mixtures being studied. In addition, the GC-SAFT-VR approach accurately captures the experimentally observed azeotropic behavior; however, as temperature increases the deviations between the predicted azeotrope vapor pressure and experimental data increases, with the azeotrope being slightly under-predicted.

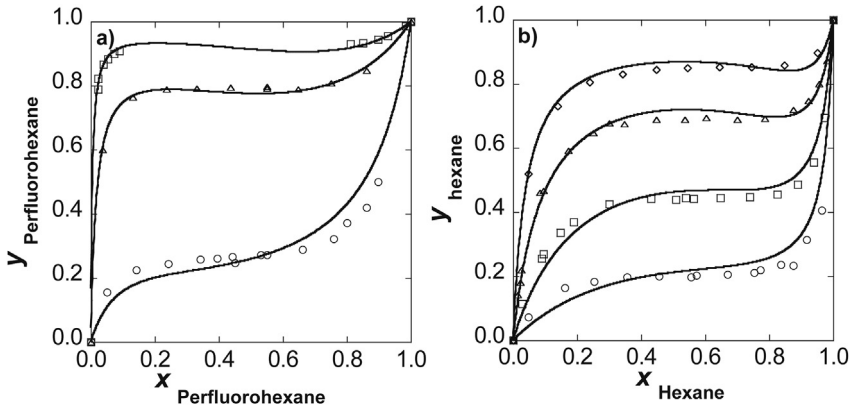

Fig. 3. Predicted composition curves for a.) perfluorohexane + pentane (circles), + heptane (triangles) and + octane (squares), and b.) hexane + perfluoropentane (circles), + perfluorohexane (squares), + perfluoroheptane (triangles) and + perfluorooctane (diamonds). Solid lines represents GC-SAFT-VR predictions and the data points represent experimental data [21].

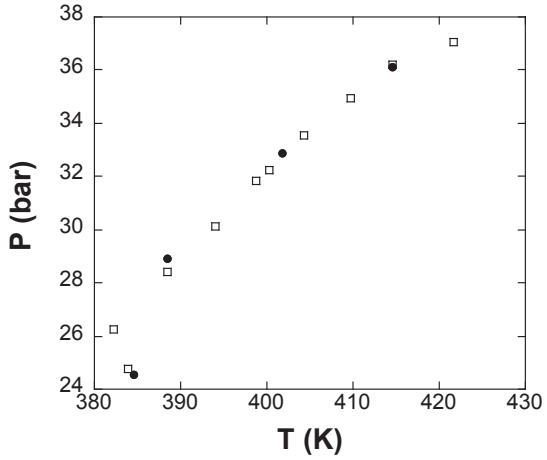

Fig. 4. Predicted *pT* projection of the critical line for the butane (1) + perfluorobutane (2) binary mixture. Black circles represent predictions from the GC-SAFT-VR approach and open squares show results from the SAFT-VR [18] equation.

In Fig. 5b, a constant temperature *Pxy* slice of the perfluorohexane + pentane binary mixture is predicted at 293.15 K. Although a slight over prediction in vapor pressure is observed near the azeotrope, improved agreement with experimental data for the vapor pressure as compared to the work of Dias et al. [21] is observed.

Additionally, we find that the theory is able to capture the change in phase behavior as the length of the perfluoroalkane is increased from perfluorohexane to perfluorooctane as shown in Fig. 6. Here we examine the *Txy* representation of the perfluorooctane + perfluoro-2-methylpentane phase diagram. For this branched fluorinated alkane we observe good agreement with experimental data in the vapor pressure predictions; however, we

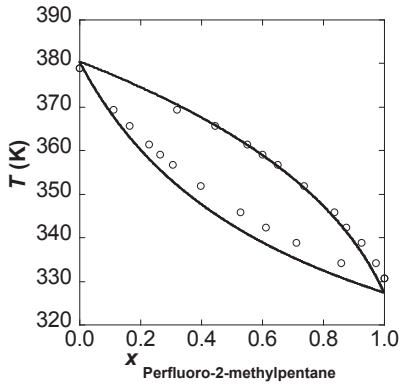

Fig. 6. Predictions of the *Txy* phase diagram for perfluorooctane + perfluoro-2-methylpentane 1.013 bar. The solid lines correspond to the theoretical predictions and the symbols the experimental data [49].

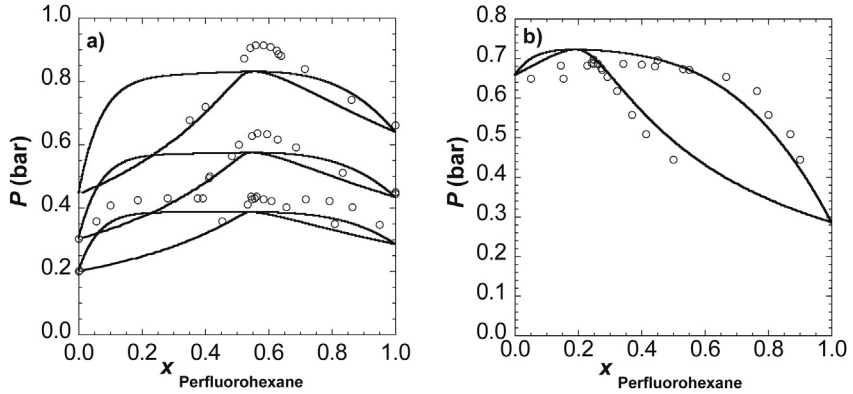

Fig. 5. *Pxy* prediction of a) perfluorohexane + hexane binary mixtures at 298.15 K, 308.15 K, and 318.15 K (bottom to top) and b) perfluorohexane + pentane binary mixture at 293.65 K. The lines correspond to the GC-SAFT-VR predictions and the symbols the experimental data [20,48].

see slight deviations in the liquid predictions, particularly at lower temperatures. Nonetheless, considering this mixture has been predicted with no fitting to binary mixture data, we consider the results to be very good.

We now consider in Fig. 7 the phase behavior of the binary mixture of perfluorobutane with butane and butene. Constant temperature *Pxy* slices of the phase diagram for the perfluorobutane + butane binary mixture are presented in Fig. 7a. Both M^{c}Cabe et al. [18] and Aparicia [50] have previously studied this mixture, with the results also in good agreement with experimental data, however fitted cross interactions were used. In the case of butene, the presence of the double bond results in deviations from Lorentz-Berthelot behavior; however, in this case pure fluid data is not available to determine the correct interaction between the CH_2 =CH and CF_2 groups. Therefore, the interaction between CH_2 = CH and CF_2 was fitted to experimental mixture data

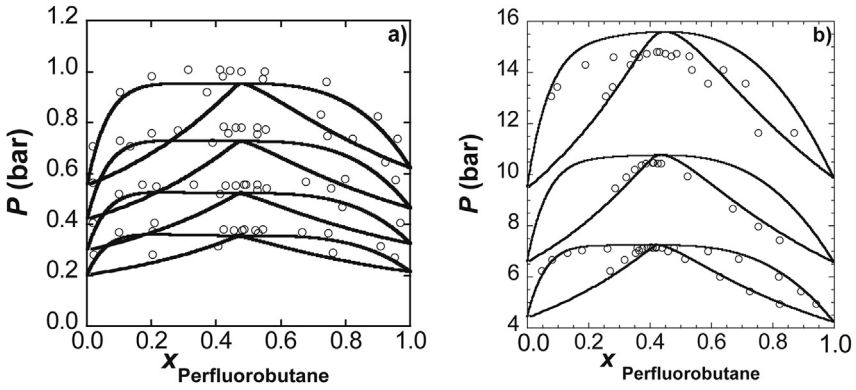

Fig. 7. a.) *P-x-y* diagram at 259 K, 253 K, 246 K, and 238 K (top to bottom) of perfluorobutane + butane binary mixtures. b.) *P-x-y* diagram at 342 K, 327 K and 312 K (top to bottom) of perfluorobutane + butene binary mixtures. Solid lines represent results from the GC-SAFT-VR approach while the experimental data points [51] are represented by open circles.

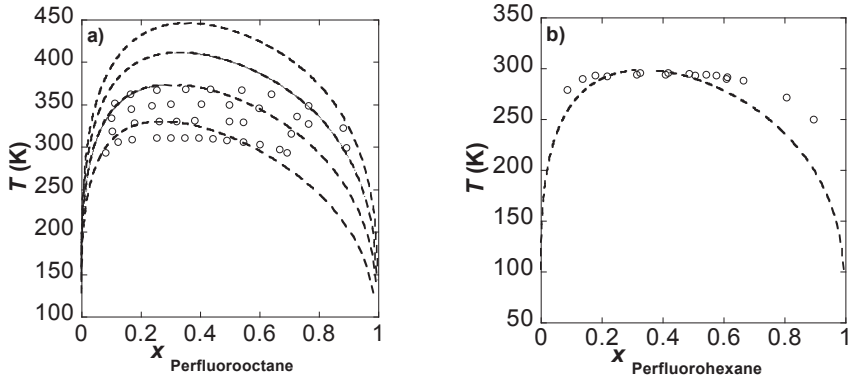

Fig. 8. a.) LLE diagram at a constant pressure of 1.013 bar for binary mixtures of perfluorooctane + alkanes, hexane, heptane, octane and nonane (from top to bottom). Solid lines represent predictions from the GC-SAFT-VR approach and open circles represents the experimental data points [52]. b.) LLE diagram at a constant pressure of 1.013 bar for the binary mixture of perfluorohexane + hexane. The solid line represents the theoretical prediction and the open circles represent the experimental data [52].

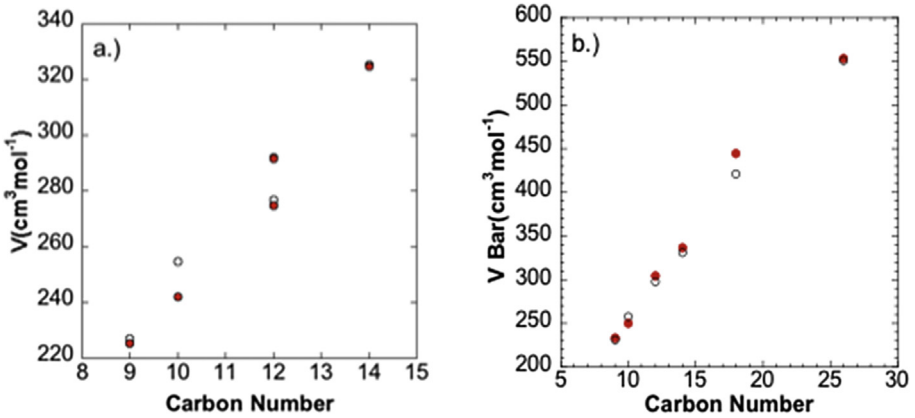

Fig. 9. a.) Molar volume as a function of carbon number for PFAA and octane binary mixtures. b.) Partial molar volume as a function of carbon number for PFAA and octane binary mixtures. Open circles represent the theoretical predictions and the red circles the experimental data [26,27]. (For interpretation of the references to colour in this figure legend, the reader is referred to the web version of this article.)

at 312 K and used in a transferable manner to predict the phase behavior at 327 K and 342 K. We note that although agreement between experimental results and predictions are good, at higher temperatures, the pressure is slightly over-predicted. Fig. 7b shows the *Pxy* representation for the perfluorobutane + butene binary mixture at three constant temperature slices of 342 K, 327 K and 312 K.

In addition to presenting information on VLE, the liquid-liquid equilibrium (LLE) of binary mixtures of PFAs and alkanes has also been studied. Specifically, the symmetric mixture of perfluorohexane + hexane as well as binary mixtures of perfluorooctane + alkanes from hexane to nonane. For these systems, the theoretical predictions are in good agreement with the experimental data and able to capture the increase in upper critical solution temperature (UCST) with increasing molecular weight of the alkanes as shown in Fig. 8a. As can be seen from the figure, the GC-SAFT-VR equation over predicts the UCST in most cases, especially for the longer alkane chains, which is consistent with the work of Dias et al. [21] where over-prediction of the UCST was observed for all systems. We note that Colina et al. [47], avoided the discrepancy found in the critical region by rescaling the model parameters to the critical point. Finally in Fig. 8b predictions for the symmetric mixture perfluorohexane + hexane are presented and found to be similar in accuracy to the work of Morgado et al. [20]; however, Morgado fitted to the perfluorohexane + hexane mixture in order to determine the appropriate cross interactions.

As an additional test of the fluorinated group parameters, the apparent molal volumes, $V_{\phi,}$, of several PFAA and alkane binary mixtures have been investigated. In the work of Morgado et al. [26], the apparent molal volumes, $V_{\phi,}$, of the solutes in all solutions was measured and then calculated from the equation:

$$V_{\phi} = \frac{M_w m_{solvent}\rho^0 - M_w m_{solvent}\rho}{m_{solute}\rho\rho^0} + \frac{M_w}{\rho} \tag{12}$$

where M_w is the molecular weight of the solute, $m_{solvent}$ and m_{solute} are the masses of the solvent and solute, and ρ^0 and ρ are the densities of the pure solvent and solution, respectively. In Fig. 9a and b, the theoretical results for the molar and partial molar volumes respectively are compared with experiment [26,27] as a function of carbon number. We observe good agreement between the experimental data and theoretical predictions for all mixtures; though we note in Fig. 9a for F4H6 the theory over predicts the molar volume, though the deviation is still only 5.0% and could be further reduced with the introduction of additional cross interactions. Morgado et al. [26] obtained similar results to those shown here, though we note again that the results presented here were predicted without the need to fit cross interactions to experimental mixture data.

Finally, due to the importance and application of systems involving CO_2 and fluorinated molecules, systems involving CO_2 were also studied. The SAFT-VR CO_2 parameters were taken from the literature [53,54] and are provided in Tables 1–3. Using the CO_2, CF_3, and CF_2 parameters, the GC-SAFT-VR approach was then used to determine the phase behavior of the CO_2 + perfluorohexane and CO_2 + perfluorooctane mixtures. Fig. 10a and b shows a *Pxy* slices of the CO_2 + perfluorohexane and CO_2 + perfluorooctane phase diagrams respectively. In addition, *Txy* slices of the CO_2 + 1,1,2,3,3,3-hexafluoropropyl (2,2,2-trifluoroethyl) ether binary mixture was predicted as shown in Fig. 10b. In all cases excellent predictions are obtained with the use of a single fitted cross interaction between the CO_2 molecule and CF_2 group. The perfluorooctane + CO_2 binary mixture at 333.15 K was used to determine the cross interaction, with all other systems in Fig. 10 then predicted; note the use of a binary mixture to fit the cross interaction is unavoidable since the

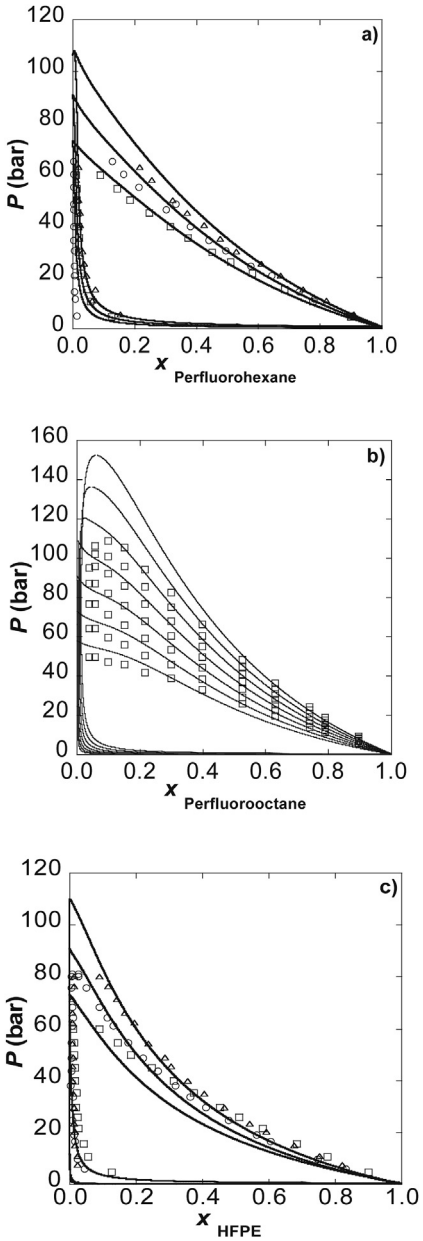

Fig. 10. Constant temperature *Pxy* slices of CO_2 + a) perfluorohexane binary mixture at 303.15 K (squares), 313.15 K (circles), and 323.15 K (triangles), b) perfluorooctane at 293.15 K, 303.15 K, 313.15 K, 323.15 K, 333.15 K, 343.15 K, and 353.15 K (bottom to top) and c) $C_5H_3F_9O$ at 303.15 K (squares), 313.15 K (circles), and 323.15 K (triangles). Solid lines represent the GC-SAFT-VR predictions and the symbols the experimental data [21].

CO_2 molecule cannot be treated within the group contribution approach. We note that for the systems in Fig. 10, Dias et al. [21] found similar results with the soft-SAFT equation of state by implementing two fitted binary interaction parameters. Thus, we are able to reduce the number of fitted interactions, whilst increasing the accuracy of the approach.

4. Conclusions

In this work, the GC-SAFT-VR approach has been expanded to include the groups required to model organofluorine molecules. Several new functional groups (CF_3, CF_2, CF, CH_2F, CHF_2, and CHF) have been defined in order to describe the fluorinated molecules of

interest by fitting to experimental vapor pressure and saturated liquid density data for selected fluorinated molecules within each class of molecule studied. The parameters are then used in a transferable fashion to predict the phase behavior of other molecules not included in the fitting process. We find from electron density maps for PFAA molecules that the electron density is greatest at the CH_2 - CF_2 junction and was taken into account in the model in order to develop an accurate GC approach for PFAA molecules.

With parameters for pure PFAs, PFAAs and HFEs developed both the VLE and LLE of mixtures of these substances and with CO_2 were studied and in general good agreement with experimental observations obtained. The transferability of the parameters was thus demonstrated and is an example of one of the advantages of utilizing a group contribution approach. We also note that as a result of the heteronuclear nature of the GC-SAFT-VR group contribution approach, an improvement is seen in the predictive ability for mixtures of PFA and PFAA as compared to other SAFT approaches.

Acknowledgments

We gratefully acknowledge financial support from the National Science Foundation under Grant CBET-1067642 and the U.S. Department of Energy (DOE), Office of Basic Energy Sciences, Geoscience Research Program, through Grant No. ERKCC72 of Oak Ridge National Laboratory, which is managed for DOE by UT Battelle, LLC under Contract No. DE-AC05- 00OR22725. Jessica Haley also acknowledges support from the U.S. Department of Education for a Graduate Assistance in Areas of National Need (GAANN) Fellowship under grant number P200A090323.

Appendix A

Table A.1
Average absolute deviation in vapor pressures and saturated liquid densities obtained between experimental data and theoretical results for pure fluorinated fluids. *Molecule used to determine the model parameters.

Compounds	T (K)	N_{pt}	%AAD*P*	%AADρ_{liq}
Perfluoroalkanes				
Perfluoropropane	241–383	13	6.92	1.21
Perfluorobutane*	154–345	20	5.11	2.69
Perfluoropentane*	170–370	21	4.10	2.96
Perfluorohexane	185–395	43	4.01	2.49
Perfluoroheptane*	225–425	41	4.34	2.05
Perfluorooctane*	250–445	40	3.51	1.08
Perfluorononane	375–445	15	8.36	1.79
Perfluorodecane*	310–500	39	2.22	1.65
Average			4.82	1.99
Perfluoroalkylalkanes				
Perfluorobutylpentane*	P:278–327	P:27	3.81	
	ρ_{liq}:278–353	ρ_{liq}:16		0.55
Perfluorobutylhexane	P:278–327	P:23	3.11	
	ρ_{liq}:278–353	ρ_{liq}:16		0.62
Perfluorobutyloctane	P:297–327	P:17	3.01	
	ρ_{liq}:278–353	ρ_{liq}:16		0.64
Perfluorohexylhexane*	P:288–327	P:20	10.34	
	ρ_{liq}:278–353	ρ_{liq}:16		0.15
Perfluorohexyloctane	ρ_{liq}:278–353	ρ_{liq}:16		0.23
Average			5.07	0.44
Branched Fluorinated Alkanes				
2-Fluoro-2-methylbutane*	250–340	25	0.74	1.55
Average			0.74	1.55
1,1-Difluoralkanes				
F_2-$(CH)_xCH_3$				
1,1-Difluoropentane*	270–375	22	8.34	0.13
1,1-Difluorohexane*	290–405	24	4.92	0.07
1,1-Difluoroheptane	293–425	27	9.50	0.13
1,1-Difluorooctane	300–429	44	10.01	
Average			8.19	0.11
1-Fluoroalkanes				
F-$(CH_2)_xCH_3$				
1-Fluoropentane	250–370	32	9.99	0.18
1-Fluorohexane	290–425	32	4.84	0.10
1-Fluoroheptane*	290–425	32	0.81	0.35
1-Fluorooctane*	290–445	38	3.79	0.56
1-Fluorononane	293–470	37	6.69	0.45
Average			5.22	0.30
Branched Fluorinated Alkanes				
2- Fluoropropane	173–325	35	4.96	2.51
2-Fluorobutane	253–385	32	5.04	1.12
3-Fluorohexane*	280–395	24	4.88	0.96
Average			4.96	1.53
Hydrofluoroethers				
HFE-347pc-f	297–463	19	11.54	
HFE-347mcf*	298–455	16	4.05	
HFE-356mf-f*	293–393	24	0.21	
HFE-374pcf	342–505	20	2.22	
HFE-449mec-f*	302–475	19	7.68	
HFE-449mcf-c	299–473	21	1.45	
HFE-458pcf-c	322–509	19	11.53	
HFE-467mccf*	291–481	23	0.74	
HFE-569mccc	280–395	24	2.00	
Average	309–453	15	4.60	

The average absolute deviations in pressure and liquid density expressed using *AAD P* (%) and *AAD* ρ_{liq} (%) are given by following equations,

$$AAD\ \ P(\%) = \frac{1}{N_{pt}} \sum_{i=1}^{N_{pt}} \left| \frac{P_i^{theo} - P_i^{\exp}}{P_i^{\exp}} \right| \times 100\%$$

$$AAD\ \ \rho_{liq}(\%) = \frac{1}{N_{pt}} \sum_{i=1}^{N_{pt}} \left| \frac{P_i^{theo} - P_i^{\exp}}{P_i^{\exp}} \right| \times 100\%$$

where $P_i^{\exp}$ and P_i^{theo} are the experimental and calculated pressure; $\rho_i^{\exp}$ and ρ_i^{theo} are the experimental and calculated saturated liquid density, respectively and N_{pt} is the number of experimental points being evaluated.

References

[1] B. Betzemeier, P. Knochel, Perfluorinated solvents - a novel reaction medium in organic chemistry, in: Modern Solvents in Organic Synthesis, Springer-Verlag Berlin, Berlin, 1999, pp. 61–78.
[2] G. Lewandowski, E. Meissner, E. Milchert, Special applications of fluorinated organic compounds, J. Hazard. Mater. 136 (2006) 385–391.
[3] G. Sandford, Perfluoroalkanes, Tetrahedron 59 (2003) 437–454.
[4] M. Pilarek, Liquid perfluorochemicals as flexible and efficient gas carriers applied in bioprocess engineering: an updated overview and future prospects, Chem. Process Eng. 35 (2014) 463–487.
[5] M.P. Krafft, Fluorocarbons and fluorinated amphiphiles in drug delivery and biomedical research, Adv. Drug Deliv. Rev. 47 (2001) 209–228.
[6] C.O. Klein, L. De Viguerie, C. Christopoulou, U. Jonas, C.G. Clark, K. Mullen, D. Vlassopoulos, Viscoelasticity of semifluorinated alkanes at the air/water interface, Soft Matter 7 (2011) 7737–7746.
[7] G. Das, M.C. dos Ramos, C. McCabe, Accurately modeling benzene and alkylbenzenes using a group contribution based SAFT approach, Fluid Phase Equilibria 362 (2014) 242–251.
[8] C. Tsagogiorgas, J. Krebs, M. Pukelsheim, G. Beck, B. Yard, B. Theisinger, M. Quintel, T. Luecke, Semifluorinated alkanes - a new class of excipients suitable for pulmonary drug delivery, Eur. J. Pharm. Biopharm. 76 (2010) 75–82.
[9] H. Meinert, T. Roy, Semifluorinated alkanes - a new class of compounds with outstanding properties, Eur. J. Ophthalmol. 10 (2000) 189–197.
[10] W.T. Tsai, Environmental risk assessment of hydrofluoroethers (HFEs), J. Hazard. Mater. 119 (2005) 69–78.
[11] W.G. Chapman, K.E. Gubbins, G. Jackson, M. Radosz, New reference equation

of state for associating liquids, Ind. Eng. Chem. Res. 29 (1990) 1709–1721.
[12] W.G. Chapman, G. Jackson, K.E. Gubbins, Phase equilibria of associating fluids: chain molecules with multiple bonding sites, Mol. Phys. 65 (1988) 1057–1079.
[13] M.S. Wertheim, Fluids with highly directional attractive forces. I. Statistical thermodynamics, J. Stat. Phys. 35 (1984) 19–34.
[14] M.S. Wertheim, Fluids with highly directional attractive forces. II. Thermodynamic pertubation theory and integral equations, J. Stat. Phys. 35 (1984) 35–47.
[15] M.S. Wertheim, Fluids with highly directional attractive forces. III. Multiple attraction sites, J. Stat. Phys. 42 (1986) 459–476.
[16] M.S. Wertheim, Fluids with highly directional attractive forces. IV. Equilibrium polymerization, J. Stat. Phys. 42 (1986) 477–492.
[17] A.L. Archer, M.D. Amos, G. Jackson, I.A. McLure, The theoretical prediction of the cricital points of alkanes, perfluoroalkanes, and their mixtures using bonded hard-sphere (BHS) theory, Int. J. Thermophys. 17 (1996) 201–211.
[18] C. M^{c}Cabe, A. Galindo, A. Gil-Villegas, G. Jackson, Predicting the high-pressure phase equilibria of binary mixtures of perfluoro-n-alkanes + n-alkanes using the SAFT-VR approach, J. Phys. Chem. B 102 (1998) 8060–8069.
[19] A. Gil-Villegas, A. Galindo, P.J. Whitehead, G. Jackson, A.N. Burgess, Statistical associating fluid theory for chain molecules with attractive potentials of variable range, J. Chem. Phys. 106 (1997) 4168–4186.
[20] P. Morgado, C. McCabe, E.J.M. Filipe, Modelling the phase behaviour and excess properties of alkane + perfluoroalkane binary mixtures with the SAFT-VR approach, Fluid Phase Equilibria 228–229 (2005) 389–393.
[21] A.M.A. Dias, J.C. Pàmies, J.A.P. Coutinho, I.M. Marrucho, L.F. Vega, SAFT modeling of the solubility of gases in perfluoroalkanes, J. Phys. Chem. B 108 (2003) 1450–1457.
[22] A.M.A. Dias, H. Carrier, J.L. Daridon, J.C. Pàmies, L.F. Vega, J.A.P. Coutinho, I.M. Marrucho, Vapor–Liquid equilibrium of carbon Dioxide–Perfluoroalkane Mixtures: experimental data and SAFT modeling, Ind. Eng. Chem. Res. 45 (2006) 2341–2350.
[23] P. Morgado, Z. Honggang, F.J. Blas, C. McCabe, L.P.N. Rebelo, E.J.M. Filipe, Liquid phase behavior of perfluoroalkylalkane surfactants, J. Phys. Chem. B 111 (2007) 2856–2863.
[24] Y. Peng, C. McCabe, Molecular simulation and theoretical modeling of polyhedral oligomeric silsesquioxanes, Mol. Phys. 105 (2007) 261–272.
[25] C. McCabe, A. Gil-Villegas, G. Jackson, F. Del Rio, The thermodynamics of heteronuclear molecules formed from bonded square-well (BSW) segments using the SAFT-VR approach, Mol. Phys. 97 (1999) 551–558.
[26] P. Morgado, H. Rodrigues, F.J. Blas, C. McCabe, E.J.M. Filipe, Perfluoroalkanes and perfluoroalkylalkane surfactants in solution: partial molar volumes in n-octane and hetero-SAFT-VR modelling, Fluid Phase Equilibria 306 (2011) 76–81.
[27] P. Morgado, R. Tomas, Z. Honggang, M.C. dos Ramos, F.J. Blas, C. McCabe, E.J.M. Filipe, Solution behavior of perfluoroalkanes and perfluoroalkylalkane surfactants in n-octane, J. Phys. Chem. C 111 (2007) 15962–15968.
[28] M.C. dos Ramos, F.J. Blas, Theory of phase equilibria for model mixtures of n-alkanes, perfluoroalkanes and perfluoroalkylalkane diblock surfactants, Mol. Phys. 105 (2007) 1319–1334.
[29] T. Lafitte, F. Plantier, M.M. Piñeiro, J.-L. Daridon, D. Bessières, Accurate global thermophysical characterization of hydrofluoroethers through a statistical associating fluid theory variable range approach, based on new experimental high-pressure volumetric and acoustic data, Ind. Eng. Chem. Res. 46 (2007) 6998–7007.
[30] J. Vijande, M.M. Pineiro, D. Bessieres, H. Saint-Guirons, J.L. Legido, Description of PVT behaviour of hydrofluoroethers using the PC-SAFT EOS, Phys. Chem. Chem. Phys. 6 (2004) 766–770.
[31] Y. Peng, K.D. Goff, M.C. dos Ramos, C. McCabe, Developing a predictive group-contribution-based SAFT-VR equation of state, Fluid Phase Equilibria 277 (2009) 131–144.
[32] Y. Peng, K.D. Goff, M.C. dos Ramos, C. McCabe, Predicting the phase behavior of polymer systems with the GC-SAFT-VR approach, Ind. Eng. Chem. Res. 49 (2010) 1378–1394.
[33] M.C. dos Ramos, J.D. Haley, J.R. Westwood, C. McCabe, Extending the GC-SAFT-VR approach to associating functional groups: alcohols, aldehydes, amines and carboxylic acids, Fluid Phase Equilibria 306 (2011) 97–111.
[34] M.C. dos Ramos, C. McCabe, On the prediction of ternary mixture phase behavior from the GC-SAFT-VR approach: 1-Pentanol + dibutyl ether plus n-nonane, Fluid Phase Equilibria 302 (2011) 161–168.
[35] J.D. Haley, C. McCabe, Predicting the phase behavior of fatty acid methyl esters and their mixtures using the GC-SAFT-VR approach, Fluid Phase Equilibria 411 (2016) 43–52.
[36] G.M.C. Silva, P. Morgado, J.D. Haley, V.M.T. Montoya, C. McCabe, L.F.G. Martins, E.J.M. Filipe, Vapor pressure and liquid density of fluorinated alcohols: experimental, simulation and GC-SAFT-VR predictions, Fluid Phase Equilibria 425 (2016) 297–304.
[37] C.-R. Hwang, Simulated annealing: theory and applications, Acta Appl. Math. 12 (1988) 108–111.
[38] Y. Peng, H. Zhao, C. McCabe, On the thermodynamics of diblock chain fluids from simulation and heteronuclear statistical associating fluid theory for potentials of variable range, Mol. Phys. 104 (2006) 571–586.
[39] P.J. Leonard, D. Henderson, J.A. Barker, Perturbation theory and liquid mixtures, Trans. Faraday Soc. 66 (1970) 2439–2452.
[40] U.J. Moller, in: A.R. Lansdown (Ed.), Lubricants in Operation, English Language Edition, VDI Verlag, Dusseldorf, 1996.
[41] T. Lafitte, D. Bessieres, M.M. Piñeiro, J.-L. Daridon, Simultaneous estimation of phase behavior and second-derivative properties using the statistical associating fluid theory with variable range approach, J. Chem. Phys. 124 (2006).
[42] J.V. Sengers, J.M.H. Levelt Sengers, Thermodynamic behavior of fluids near the critical-point, Annu. Rev. Phys. Chem. 37 (1986) 189–222.
[43] R. Dennington, T. Keith, J. Millam, GaussVIew, Semichem Inc., Shawnee Mission KS, 2009.
[44] C. Tschierske, Liquid Crystals: Material Design and Self Assembly, 2012, p. 410.
[45] L. Lepori, E. Matteoli, A. Spanedda, C. Duce, M.R. Tiné, Volume changes on mixing perfluoroalkanes with alkanes or ethers at 298.15 K, Fluid Phase Equilibria 201 (2002) 119–134.
[46] A. Maciejewski, The application of perfluoroalkanes as solvents in spectral, photophysical and photochemical studies, J. Photochem. Photobiol. A Chem. 51 (1990) 87–131.
[47] C.M. Colina, A. Galindo, F.J. Blas, K.E. Gubbins, Phase behavior of carbon dioxide mixtures with n-alkanes and n-perfluoroalkanes, Fluid Phase Equilibria 222 (2004) 77–85.
[48] K. Tochigi, T. Namae, T. Suga, H. Matsuda, K. Kurihara, M.C. dos Ramos, C. McCabe, Measurement and prediction of high-pressure vapor–liquid equilibria for binary mixtures of carbon dioxide ;n-octane, methanol, ethanol, and perfluorohexane, J. Supercrit. Fluids 55 (2010) 682–689.
[49] K. Tochigi, T. Satou, K. Kurihara, K. Ochi, H. Yamamoto, Y. Mochizuki, T. Sako, Vapor–Liquid equilibrium data for the four binary systems containing fluorocarbon, hydrofluorocarbon, and fluorinated ethers at 101.3 kPa, J. Chem. Eng. Data 46 (2001) 913–917.
[50] S. Aparicio, Phase equilibria in perfluoroalkane + alkane binary systems from PC-SAFT equation of state, J. Supercrit. Fluids 46 (2008) 10–20.
[51] S.C. Subramoney, P. Naidoo, A. Valtz, C. Coquelet, D. Richon, D. Ramjugernath, Experimental (vapour+liquid) equilibrium data and modelling for binary mixtures of decafluorobutane with propane and 1-butene, J. Chem. Thermodyn. 67 (2013) 134–142.
[52] M.J. Pratas de Melo, A.M.A. Dias, M. Blesic, L.P.N. Rebelo, L.F. Vega, J.A.P. Coutinho, I.M. Marrucho, Liquid–liquid equilibrium of (perfluoroalkane and alkane) binary mixtures, Fluid Phase Equilibria 242 (2006) 210–219.
[53] A. Galindo, F.J. Blas, Theoretical examination of the global fluid phase behavior and critical phenomena in carbon dioxide + n-alkane binary mixtures, J. Phys. Chem. B 106 (2002) 4503–4515.
[54] F.J. Blas, A. Galindo, Study of the high pressure phase behaviour of CO2+n-alkane mixtures using the SAFT-VR approach with transferable parameters, Fluid Phase Equilibria 194–197 (2002) 501–509.